

Chapter 3

Diaphragm-based Pressure Sensor Fabrication

Because the sensor is intended to operate under harsh environment such as high temperature and high pressure, therefore using materials with very the same CTE (coefficient of thermal expansion) as that of optical fiber is very important to reduce thermal induced air-gap changes and failures. Ordinary single mode optical fibers are made of fused silica. It's very straightforward to use fused silica for the ferrule and the diaphragm. Also fused silica can be micro-structurable, preferably using standard lithography process (batch fabrication).

However, all fused silica doesn't mean that the fabrication of a diaphragm-based EFPI sensor is simple. Actually, fused silica wafers or ferrules are hard to polish, and difficult to bond together, especially at low temperature. Therefore, some special techniques are investigated to fabricate sensors with fused silica wafers and ferrules.

3.1 Diaphragm-based EFPI Pressure Sensor Fabrication Process

The process of the sensor fabrication includes:

- 1) photolithography on fused silica diaphragms;
- 2) polishing fused silica ferrule end;
- 3) bonding the diaphragm and the ferrule;
- 4) and bonding the ferrule and the fiber.

The pressure sensor consists of a thin diaphragm, which deforms in response to a change in pressure. The diaphragms have been micro-machined in order to form cavities. In our experiments, the cavities are etched round, 0.5mm radius. By using deep wet etching technology, 20 or 30 micron-deep pits can be obtained in 5 hours.

The fused silica ferrule end is polished to enhance the bonding quality with the diaphragm. The surface roughness on the ferrule can cause voids or even much larger un-bonded areas.

Chapter 3. Diaphragm-base Pressure Sensor Fabrication

Bonding is usually one of the most critical issues in sensor fabrication. The bonding method will finally affect the performances of the sensor and will determine the temperature dependence directly. Though there are a lot of bonding methods available, fused silica and fused silica bonding, which also need to be at low temperature, still remains a good topic for further investigation. There are also other challenges imposed by the small size of the sensor, such as fine optical alignment and diaphragm cutting.

We chose the intermediate-layer bonding method to avoid all the above mentioned difficulties during the fabrication and fully use the currently available equipments at the Center for Photonics Technology (CPT).

3.2 Diaphragm fabrication

3.2.1 Introduction to Photolithography

Photo-litho-graphy, came from latin, light-stone-write. Photolithography is an optical means for transferring patterns onto a substrate. The basic process consists of the following steps:

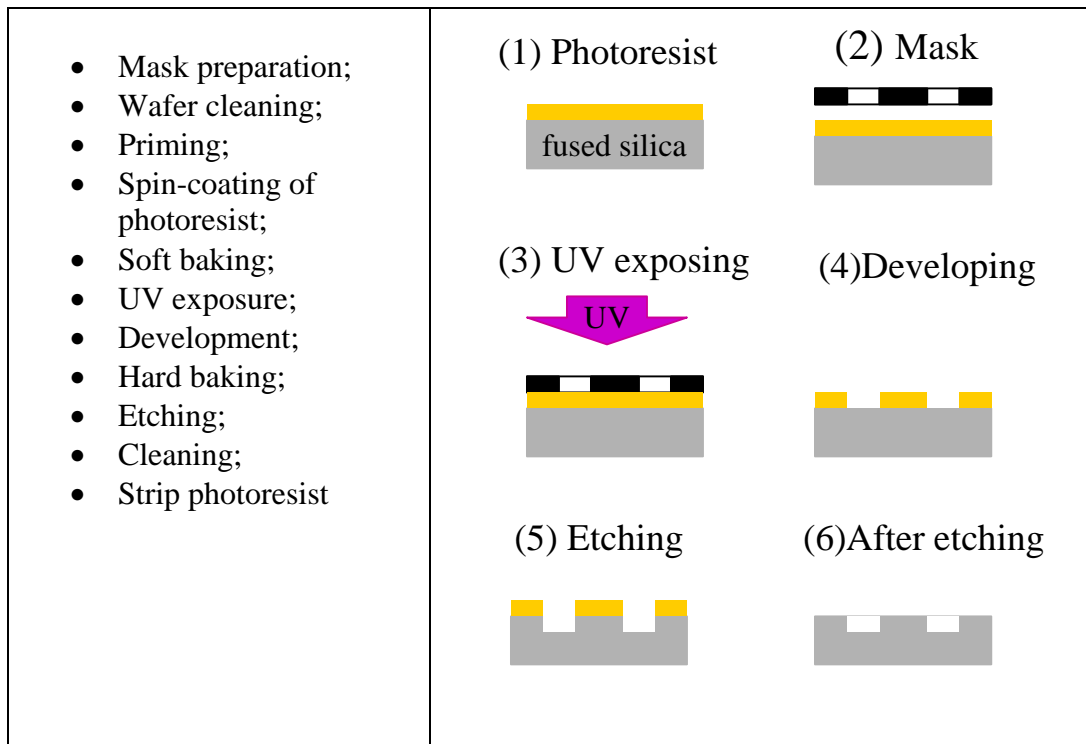


Figure 3-1 Photolithography process

Step 1. Mask preparation

A piece of copper plate or other materials that can block the UV light can be used as a mask. In this experiment, the transparency printed out with patterns is used as a mask. This is an economical mask-making method.

Step 2. Wafer Cleaning

Typical contaminants that must be removed prior to photoresist coating is:

- dust from scribing or cleaving(minimized by laser scribing);
- atmospheric dust (minimized by good clean room practice);
- abrasive particales (from lapping);
- lint from wipers (minimized by using lint-free wipers);
- photoresist residue from previous photolithography (minimized by performing oxygen plasma ashing);
- bacteria (minimized by good DI water system);
- films from other sources: solvent residue, H₂O residue, photoresist or developer residue, oil, silicon.

The standard degrease procedure is:

- 2-5 min. soak in diluted H₂SO₄ (<5%) with ultrasonic agitation
- 2-5 min. soak in DI H₂O with ultrasonic agitation
- 2-5 min. soak in acetone with ultrasonic agitation
- 30 sec. Rinse under free flowing DI H₂O
- dry with a heat gun or hotplate(~100°C)

Step 3. Priming

Primer is an adhesion promoter, used to assist photoresist coating. Hexamethyldisilazane (HMDS) is the industry's most widely used and accepted adhesion promoter. It may be applied in vapor, liquid or solution form to reduce surface energy, provide excellent surface coverage, and reduce underetch and lifting of photoresist.

HMDS (AP010 from Silicon Resources, Inc.) can be applied to substrate, spraying or dipping. Wet application is accomplished by applying HMDS directly to a wafer and

Chapter 3. Diaphragm-base Pressure Sensor Fabrication

spinning at 3000-5000rpm. Excess material is spun off and a subsequent hot plate bake (100~150°C) will complete the priming sequence. The bake temperature chosen depends on the photoresist we use. For AZ TFP 650, the priming bake temperature should be as high as 150°C.

Step 4. Spin-coating of photoresist

In this step, the fused silica diaphragm is held on a spinner chuck by vacuum and photoresist is coated to uniform thickness by spin coating.

The photoresist thickness is set by primarily photoresist viscosity, secondarily spinner rotational speed. For AZ TFP 650, the coating sequence is described in Figure 3-2.

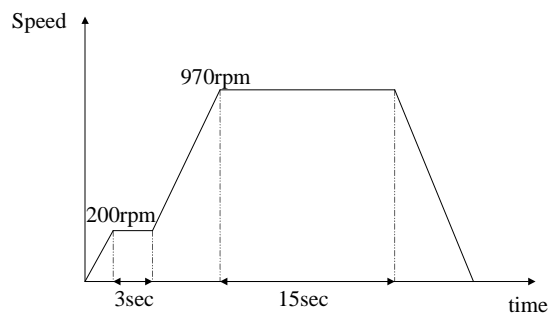


Figure 3-2 Coating sequence of AZ TFP 650

In general, we can get a photoresist film of 2~5 μm thickness. And the surface is uniform after following the coating sequence.

Step 5. Soft baking (pre-bake)

Soft baking is to reduce the solvent content in photoresist thereby increase adhesion, sensitivity and resistance to deforming forces. Hot plating the resist is usually faster, more controllable. A narrow time-temperature window is needed to achieve proper linewidth control. The thickness of the photoresist is usually decreased by 25% during prebake for both positive and negative photoresist. Less prebake increases the development rate. For photoresist AZ TFP 650, the soft baking time is 90sec, with 100°C on the hot plate.

Step 6. UV exposure and development

Align the mask to the diaphragm. The exposure by applying UV radiation decomposes a development inhibitor and developer solution only dissolves photoresist in the exposed area. The exposure time depends on the thickness of the photoresist. In general, we exposure the diaphragm for 60 seconds and immerse the diaphragm in the developer for 20 second for AZ TFP 650.

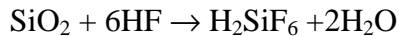
Step 7. Hard baking (post-bake)

Hard baking is to remove the solvent content in photoresist thereby increasing adhesion, hardening the photoresist and making it etch resistant. The hard baking time for photoresist AZ TFP 650 is 120 seconds with 120°C on the hot plate.

Step 8. Etching

Etching can be described as pattern transfer by chemical/physical removal of a material from a substrate, often in a pattern defined by a protective mask layer (e.g., a resist or an oxide). Mask-based etching is divided into dry etching and wet etching. Wet etching is a technique that etching is in the liquid phase. Compared to the dry etching, wet chemical etching provides a higher degree of selectivity. Wet etching often is faster and cheaper.

In our experiments, we use buffered hydrogen fluoride (BHF) as etchant. HF-based etchants are used mainly for silicon dioxide, because they were observed to etch polysilicon very slowly, but other researchers have noticed that various solutions attach polysilicon at the grain boundaries, resulting in noticeable surface roughness. Research indicates that HF can diffuse through thin polysilicon to etch underlying low-temperature oxide. For pure HF etching, the overall reaction is



HF is a weak acid, except when present in very small concentrations, it does not completely dissociate into H^+ and F^- ions in water. The etch rate of both silicon dioxide and silicon nitride increase linearly with the concentrations of both HF and HF_2^- , while being independent of the concentration of F^- ions alone. The HF_2^- complex attacks oxide

about 4.5 times faster than HF. Higher-order complexes, such as H_2F_3^- , appear to occur at higher HF concentrations (e.g. 49% HF) and attack oxide even faster than HF_2^- . Thus, the etch rate increase faster than linearly with HF concentration. ^[19]

Acidic ammonium fluoride solution is called buffered hydrogen fluoride (BHF). The chemical composition of BHF is usually a mixture of 40% NH_4F and 49% or 50% HF, ranging in weight ratios of NH_4F : HF from 5:1 to 30:1. In buffered HF solutions, for pH values above about 1, the concentration of HF_2^- is greater than that of HF. For more acidic solutions, there is sufficient hydrogen to combine with the fluoride to make HF the dominant species. As HF and HF_2^- are consumed, the etch rate decreases. Buffering with NH_4F helps keep the pH and thus the concentrations of HF and HF_2^- constant, stabilizing the etch rate. BHF is widely used as a surface treatment agent for the process of etching. ^[18]

Step 9. Cleaning and Strip photoresist

DI H_2O is used to clean the diaphragm. Rinse the diaphragm in for 2 minutes. Acetone is used to strip photoresist (PR) and for lift-off patterning of films. Lift-off processes can be sped up by heating the acetone or by placing it in an ultrasonic bath.

3.2.2 Deep wet etching on fused silica diaphragm

Following the above photolithography process, we can get a very good etched pit on the fused silica, as we can see from Figure 3-3. But the etch depth can be only up to 5 micron. Currently no photoresist can withstand BHF for long time (more than 1 hour).

In our experiment, we need to etch deeper pits to increase the dynamic range for pressure testing. The etch depth of at least 15 μm is required.

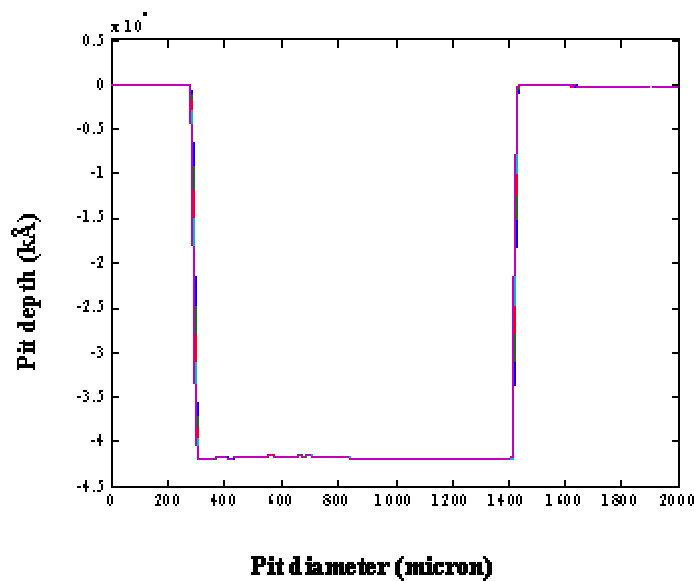


Figure 3-3 Wet etched pit on the fused silica diaphragm

3.2.2.1 Chromium layer for deep wet etching

For deeper structures, the photoresist does not withstand HF solution long enough. Thus additional masking layers that can be deposited onto glass have to be used. This mask layer should be deposited between the photoresist layer and the wafer in order to further protect the wafer surface from HF attack. We choose to use Chromium as the metal mask for several reasons:

- We have a sputtering system available for Chromium coatings;
- Chromium targets for the sputtering system are relatively cheap;
- Chromium layers can improve the adhesion of the photoresist to the diaphragm and prevent HF acid attack the diaphragm;
- Chromium layers can be easily removed by a commercial chromium mask etchant

3.2.2.2 Deep wet etch process

In order to deep etch on a fused silica diaphragm, several additional steps related with Chromium coating and Chromium layer removal are used. The whole process is shown in Figure 3-4.

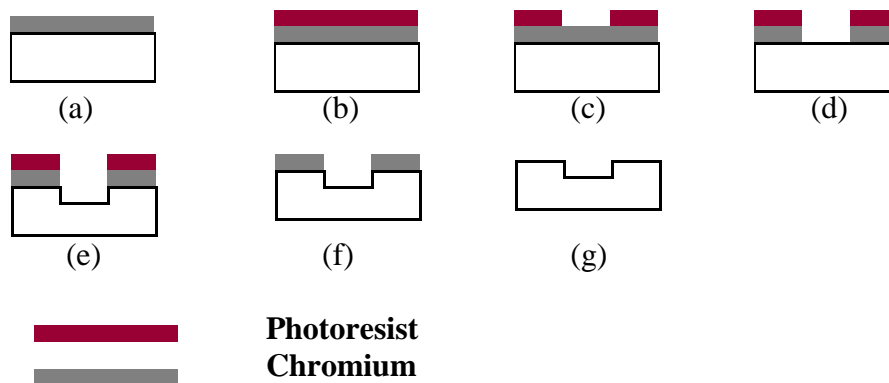


Figure 3-4 Deep wet etch process

- a) Deposit Chromium onto the diaphragm;
- b) Spin coating photoresist;
- c) UV expose and develop;
- d) Remove partial Chromium layer without photoresist protection
- e) Wet etch by BHF;
- f) Remove photoresist;
- g) Remove Chromium layer

3.2.2.3 Deposit Chromium layer by sputtering

Sputtering is a technology in which the material is released from the source at much lower temperature than thermal evaporation. The substrate is placed in a vacuum chamber with the source material, named a target, and an inert gas (such as argon) is introduced at low pressure. A gas plasma is struck using an RF power source, causing the gas to become ionized. The ions are accelerated toward the surface of the target, causing atoms of the source material to break off from the target in vapor form and condense on all surfaces including the substrate. As for evaporation, the basic principle of sputtering is the same for all sputtering technologies. The differences typically relate to the manner in which the ion bombardment of the target is realized. A schematic diagram of a typical RF sputtering system is shown in Figure 3-5. ^[4]

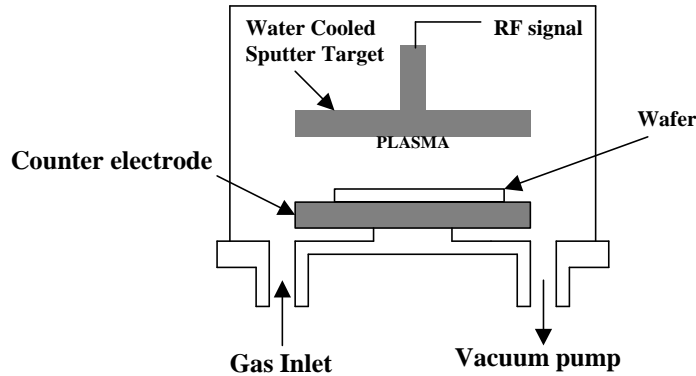


Figure 3-5 Typical RF sputtering system [4]

The coating thickness of a chromium layer depends on the RF power, the process pressure and the deposit time. The following is the results of chromium coatings at different conditions:

Power (W)	Time (Second)	Pressure (Torr)	Thickness (nm)
100	15	3.5e-3	10
100	30	3.6e-3	55
100	60	3.6e-3	70
300	60	3.4e-3	180

Table 3-1 Chromium Coating Thickness vs. Coating Conditions

3.2.2.4 Deep wet etch results

The following plot presents a diaphragm etched in BHF for 5 hours. The etched depth is about 25 micron. We can see from figure 3-6, the sidewall of the pit is still steep and the surface inside the pit is flat. Sensors made by these pits can have an interference fringe visibility as high as 98%. Even deeper pits can be etched using this method.

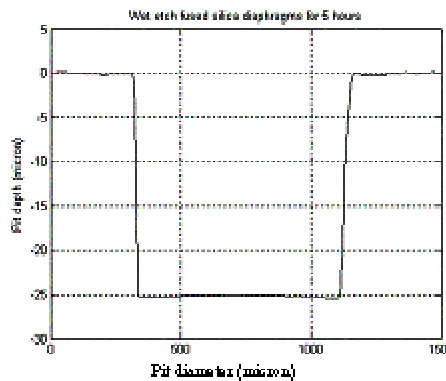


Figure 3-6 Etch result of deep wet etching

3.2.3 Two-step chemical etching on fused silica diaphragm

The center of the pit on the diaphragm is the most sensitive part. The central axis of the ferrule and the center of the pit should be aligned in order to reach the maximum sensitivity of the pressure. In Figure 3-7, a 3-D computer simulation of diaphragm deflection is presented by using Equation (2.39). In this simulation, the diameter of etched pit is 1mm, and the pressure is 800 psi, and the thickness of the diaphragm is 95 μm .

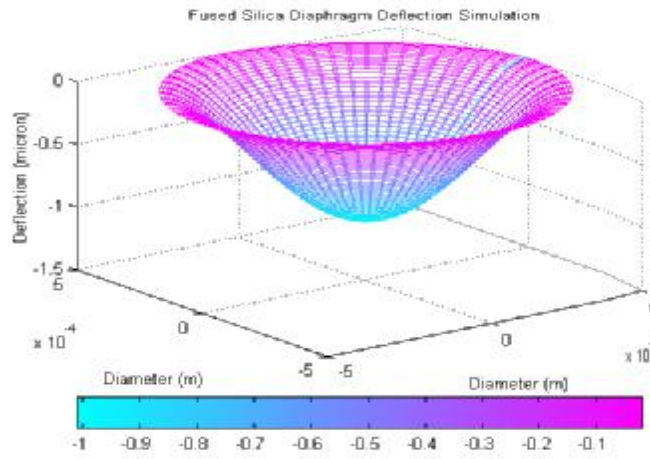


Figure 3-7 Computer simulation of fused silica diaphragm deflection

A two-step etching structure is used to make the alignment of the tube with the pit on the diaphragm easy to operate. The larger diameter is the same size of the OD of the ferrule (Figure 3-8). The ferrule can be put into the larger pit and the center of the ferrule will be automatically align with the center of the smaller etched pit which forms the interference cavity with the fiber end inserted into the ferrule.

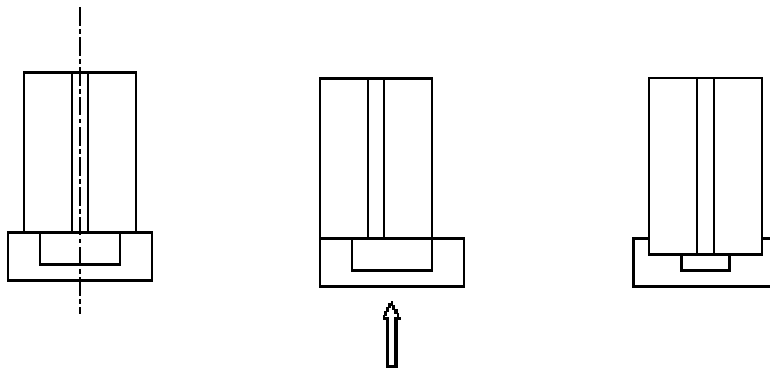


Figure 3-8 Two step etch to solve alignment problem

3.2.3.1 Two Step wet etching process

The process starts with the deposition of a 70nm Chromium layer on the fused silica diaphragm. The chromium layer is used to improve the adhesion of photoresist and results in deep etch depth. From (b) to (f) and from (g) to (l), the normal photolithography process has been used twice with two different size photo-masks. ^[18]

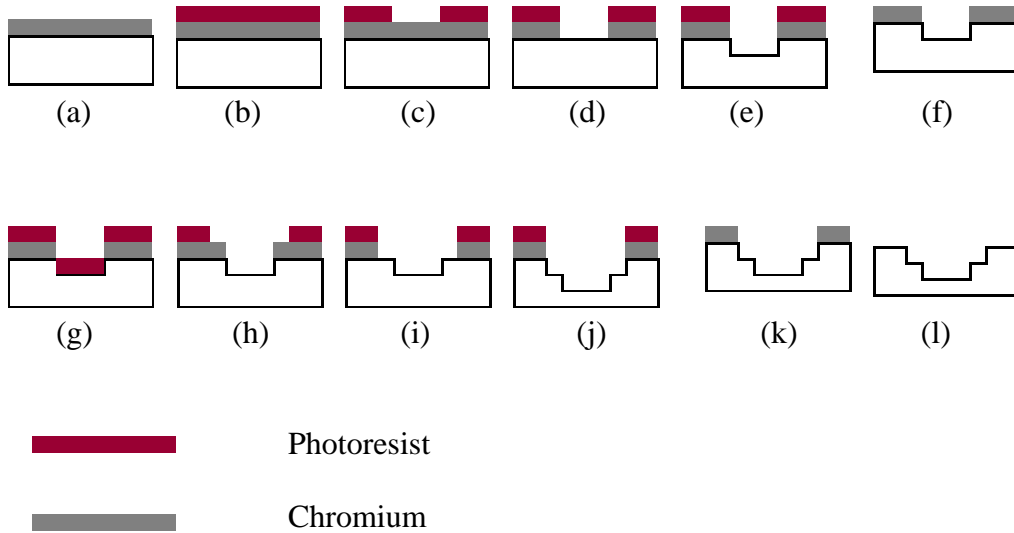


Figure 3-9 Two step wet etch process

3.2.3.2 Two step etch result

Figure 3-10 is the two-step wet etched pit observed under the profiler.

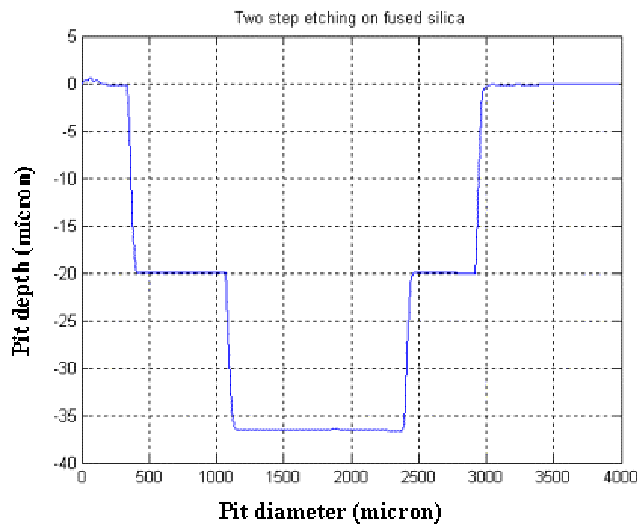


Figure 3-10 Two step wet etch result

3.2.4 Wet chemical etch results analysis

3.2.4.1 Etch rate

The wet etch rates can vary for reasons that are usefully divided into three groups: the etch setup, the material being etched, and the layout and structure on the substrate. The most significant effects on wet-etch rates are as follows:

- Temperature;
- Impurities in or on the material being etched;
- Contamination

For fused silica, the etch rate in 5:1 BHF at the room temperature is about 46.42nm per minute.

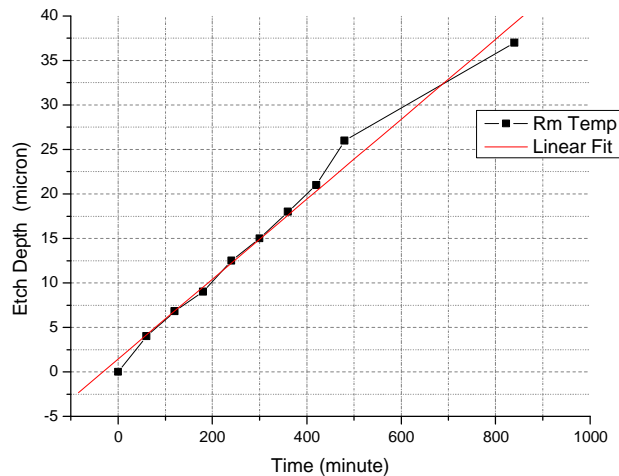


Figure 3-11 Etch rate of 5:1 BHF

If we choose to use the commercially available BHF etchant (Sigma Aldrick, Ammonium fluoride-hydrofluoric acid mixture, 35.1% NH_4F , 6.3% HF), the etch rate on fused silica at room temperature is 83.3nm per minute.

We can also notice that the total etch rate curves are not linear. After certain amount of time, the etch rate decreased a little. As we mentioned in previous sections, HF molecules and HF_2^- ions are consumed with time and make the HF concentration smaller than it was at the very beginning. If we do want to etch a sample in BHF solution for long time, bigger container with more BHF solution is suggested.

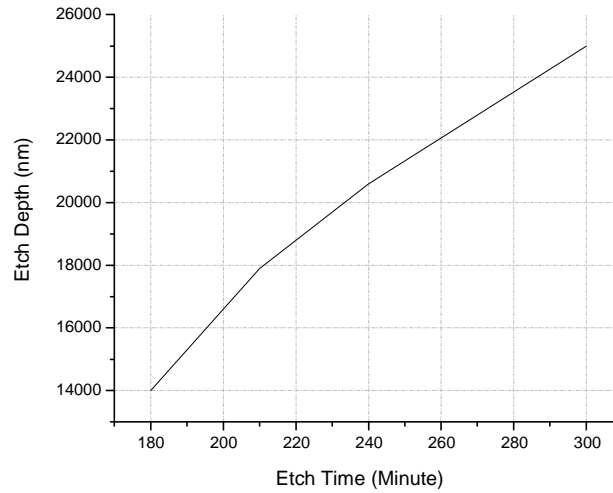


Figure 3-12 Etch rate of commercial BHF

3.2.4.2 Surface roughness

The amount of ammonium fluoride (NH_4F) in BHF solution is the most important factor that affected the surface cleanness. Some pin holes appeared on the etched diaphragm if we didn't mix enough with NH_4F . The smoothness of the surface can be ensured through wet etching by the improvement of the compositions of the BHF solution. For the left plot in Figure 3-13, we mix H_2O , HF_4F and HF with the percentage of 58%: 20%:22% and for the right plot in Figure 3-13, the concentration ratio changed to be: H_2O : NH_4F : HF = 58%:36%:6%. We can see from the two plots in Figure 3-13 that the surface quality in the second plot is significantly improved by changing BHF composition.

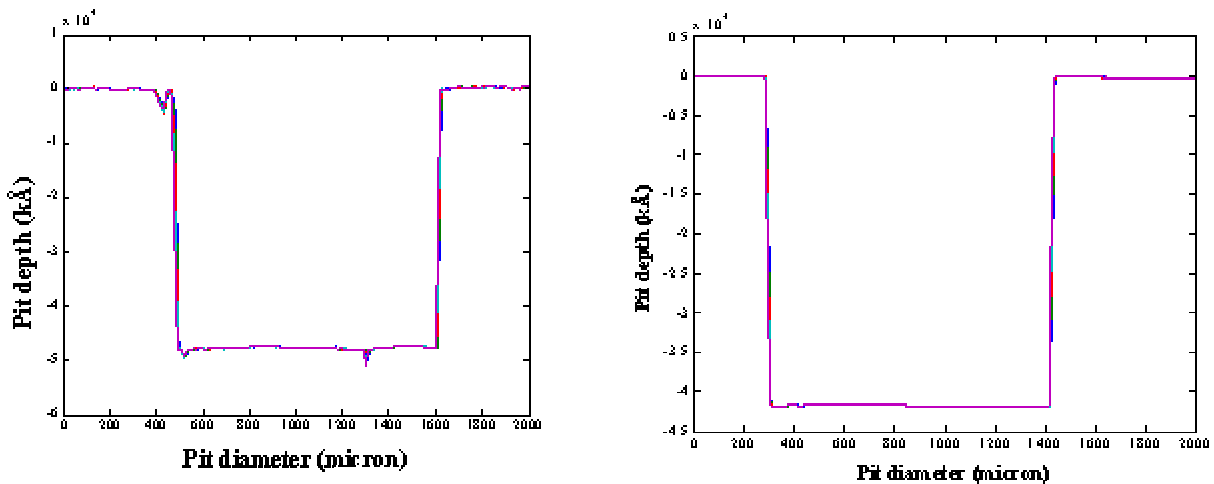


Figure 3-13 Surface quality improvement

Chapter 3. Diaphragm-base Pressure Sensor Fabrication

Also, the lower concentration of the HF, the better surface quality we can get. So chemical etching is a possible means to mitigate the growth of surface damage on fused silica.

There is a trade-off between surface quality and etch rate. For our sensor fabrication, we finally choose commercially available BHF with higher concentration to etch the small size pit. The etch rate is high and we can get as deep as 20 μm pits in 4 hours. But the etched surface became a little bit rough after so long time etching as shown in Figure 3-13 (2nd plot). Then we used 10:1 BHF to etch the larger size pits. Since we don't care much about the depth of the larger pits and lower concentrate of HF can mitigate the surface roughness of the small pits caused by the first etch process.

The reflectance of the etched pit on the fused silica diaphragm can be as high as 4% with normal light incidence.

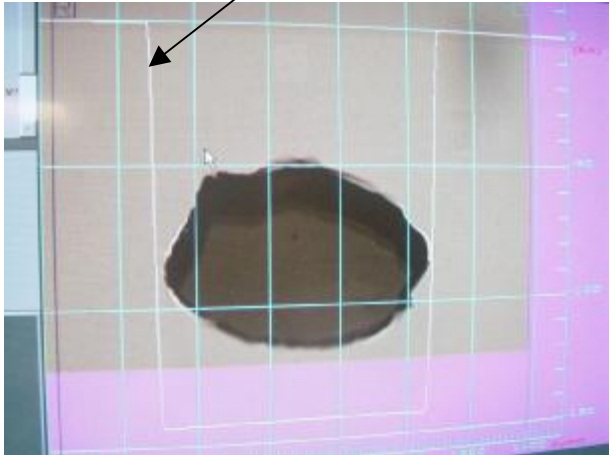
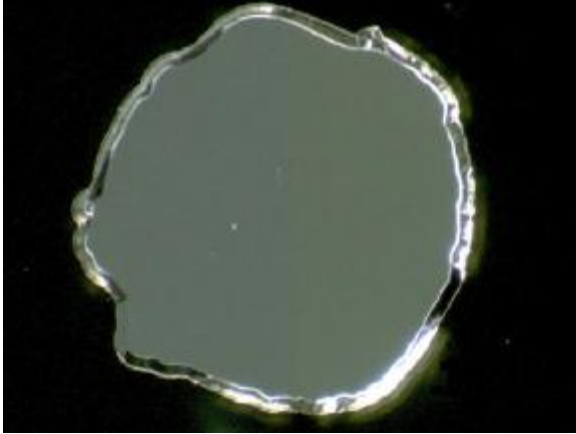
Picture from Surface Profiler	Picture from Microscope
<p data-bbox="375 1010 781 1083">White curve is the scan result of the etched pit</p> 	<p data-bbox="948 1010 1208 1083">Black area is Chromium coating</p> 

Table 3-2 Pictures of Etched Pit

3.2.4.3 Diameter Deviation

The main factor that affects the diameter of the etched pit is the UV exposure process including the distance between the UV light source and the substrate and the exposure time. Ideally, different areas of the substrate should be exposed by the same energy and

the same period. If we put the UV light too close to the substrate (Figure 3-14, left), some areas were over-exposed and some other areas were under-exposed because of the limited size of the UV light. This caused the diameter of the size to vary a lot.

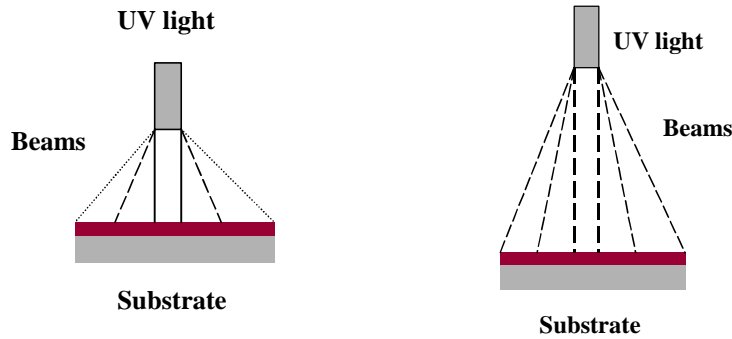
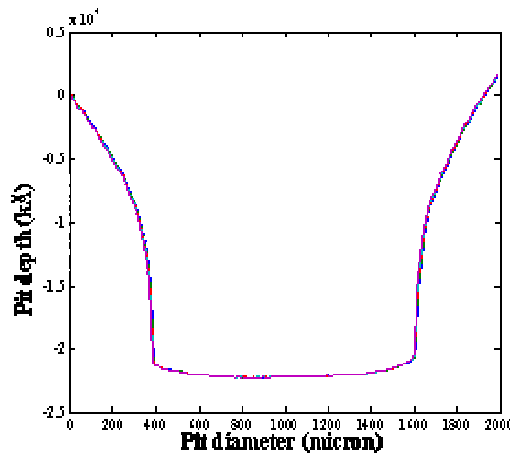


Figure 3-14 UV light exposure

If we place the UV light source far away from the substrate, the exposure would be more uniform as illustrated in Figure 3-14 (right plot). But longer exposure time is needed. In this experiment, the distance between the UV light and the substrate is 8 cm and the exposure time is 4 minutes.

The other factor that has some effects on the diameter size is the etching process. We can see from the plot in Figure 3-15 that the sidewalls of the 2nd pit are very straight and smooth. Therefore, the deviations of the etched pit diameter are reduced. We can see that in the second plot the diameter deviation is: $(1.14-1.04)/1.04*100\%=9.6\%$, but in the first plot, the diameter deviation is: $(1.8-1.04)/1.04*100\%=73\%$. The sensitivity of the sensor can be better controlled with the reduced deviation of the pit diameter per our calculation in the diaphragm design section.



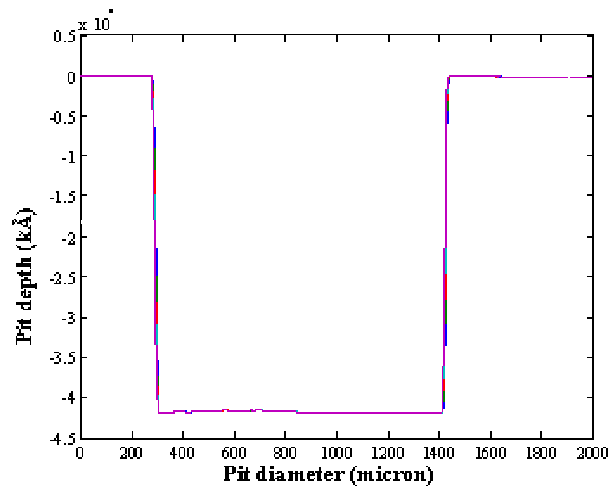


Figure 3-15 Diameter Deviation

3.2.4.4 Etch depth uniformity

Figure 3-16 shows two etched pits on two different diaphragms measured by a surface profiler. These two diaphragms were both etched in the commercial BHF for 5 hours respectively. The etch depth was controlled by BHF concentration, the temperature and the time. Since HF is extremely dangerous, we normally only use it under the room temperature. And commercial BHF is used in order to keep the BHF concentration unchanged. Figure 3-17 shows six etched pits on the same diaphragm measured by a surface profiler.

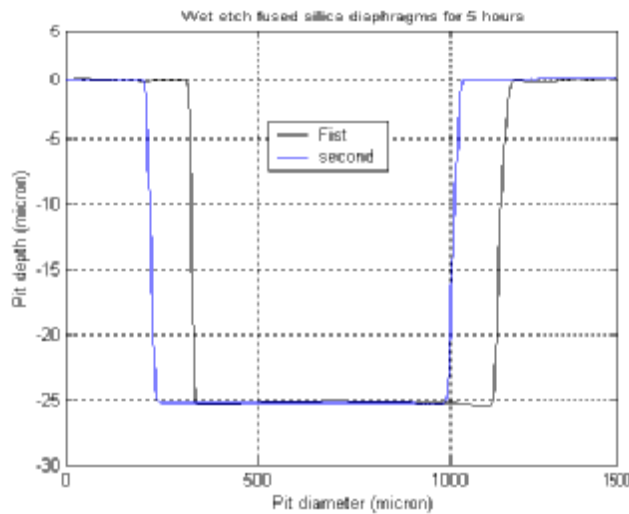


Figure 3-16. Etched pits on two different diaphragms

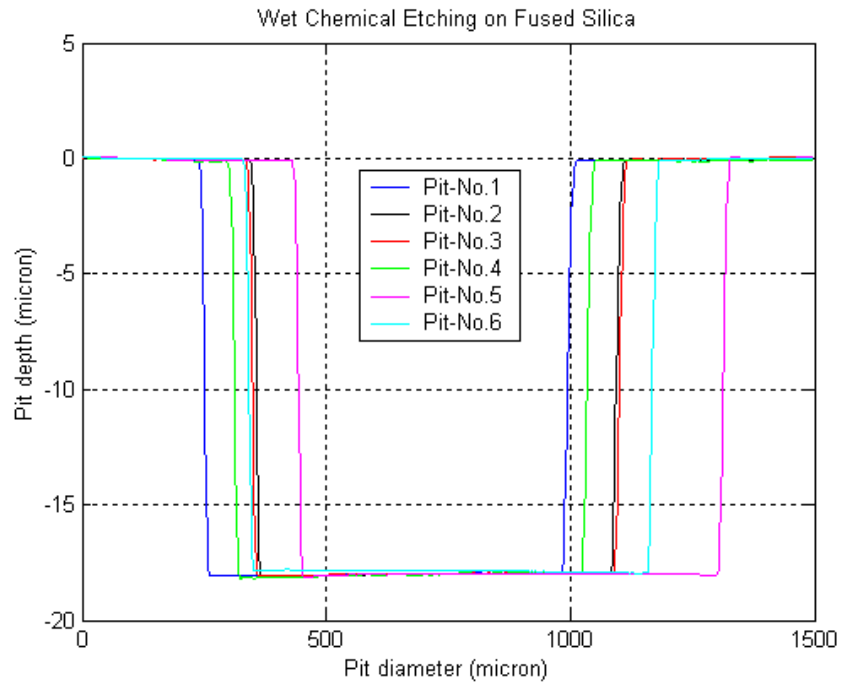


Figure 3-17 Etched pits on the same diaphragm

3.3 Bonding

3.3.1 Introduction to bonding technology

MEMS are shrinking sensors and actuators into micro- and nanometer scales while micropackaging emerges as the bottleneck for successful device commercialization.^[21] The existing MEMS packaging technologies includes packaging and bonding. Bonding provides at least two functions for sensor fabrication: mechanical support and thermal management.

General bonding technology can be divided into two major branches: Direct bonding and intermediate layer bonding. Fusion bonding and anodic bonding are known as direct bonding. Spin On Glass (SOG) thermal bonding, Eutectic bonding, Solder bonding, and organic layers bonding are known as intermediate layer bonding.

The invention of anodic bonding dates back to 1969 when Walls and Promerantz found that glass and metal can be bonded together at about 200-400 °C below the melting point of glass with the aid of a high electrical field. Unfortunately, the possible contamination

Chapter 3. Diaphragm-base Pressure Sensor Fabrication

due to excessive alkali metal in the glass; possible damage to microelectronics due to the high electrical field; and the requirement of flat surface for bonding limit the application of anodic bonding to MEMS. Furthermore, for our sensor fabrication, anodic bonding cannot be applied because this method cannot work between fused silica and fused silica.

Fusion bonding is mostly used in silicon-on-insulator (SOI) technology such as Si-SiO₂ bonding and silicon-silicon bonding. It is a proven method and the bonding strength is enormously strong. Unfortunately, since the temperature requirement is generally higher than 1000°C, it may not be suitable for our sensor fabrication because the gold coating on both interference cavity surfaces may have to be used to improve the reflectance. Such a high temperature can severely damage the gold coating films.

Eutectic bonding, which is based on the use of bonding materials that form a eutectic alloy in specific temperature conditions, has been used widely in microfabrication. It provides high bonding strength and good stability at a relatively low bonding temperature at 363°C. But this method is difficult to obtain complete bonding over large surface areas, and even native oxides prevent bonding from taking place and eutectic bonding is reported to introduce substantial mounting stress in piezoresistive sensors, causing long-term drift due to relaxation of the built-in stress.

Solder bond technology is widely used in the connection to chip process in IC packaging. Solders are often used to bond two metals together in electrical engineering. Because solders have reasonably good mechanical strength, the bonding is usually solid and stable. The disadvantage of solder bonding is that most of the solder cannot withstand high temperature.

There are also some other intermediate layer bonding technologies, such as: SOG thermal bonding, Epoxy bonding and Intermediate layer borosilica glass bonding. All the intermediate layer bonding methods have the same disadvantage that the coefficients of thermal expansion and Young's modulus of the intermediate layer material are different from that of the fused silica components in the sensor. This difference causes very poor temperature stability of the sensor and bonding is not really physically 'solid'.

3.3.2 SOL-GEL intermediate layer bonding

It seems that, the direct bonding of a fused silica ferrule and a fused silica diaphragm is the most promising way to reduce the temperature dependence. However, there are two reasons not to choose the direct bonding.

It is well known that “intimate contact” and “temperature” are two major factors for direct bonding “Intimate contact ” puts two separated surfaces together and “temperature” provides the bonding energy.

On intimate contact, though we can successfully bond two fused silica wafers together, directly bonding a patterned diaphragm to a flat substrate, directly bonding a patterned diaphragm and a ferrule still faces a number of challenges and is currently under investigation at the Center for Photonics Technology.

On temperature side, fusion bonding and anodic bonding require high temperatures that may damage the gold coatings we may have to use to increase the reflectance.

Using the intermediate layer bonding seems a natural choice in our research. Sol-gel is chosen to be as the intermediate layer for several reasons:

- Sol-gel is a low temperature process;
- Thin films can be formed by sol-gel process;
- The final form of sol-gel process “gel” can be high purity silica, which will reduce the thermal expansion of the intermediate layer;
- Sol-gel can be made in our lab and it is a cheap process

In our reseach, sol-gel is used for both the diaphragm-to-ferrule bonding and the ferrule-to-fiber bonding.

3.3.2.1 SOL-GEL process

The term sol-gel was first coined in the late 1800s. It generally refers to a low-temperature method using chemical precursors that can produce ceramics and glasses

with better purity and homogeneity than high temperature conventional processes. In general, the sol-gel process involves the transition of a system from a liquid “sol” (mostly colloidal) into a solid “gel” phase (usually silica). Applying the sol-gel process, it is possible to fabricate ceramic or glass materials in a wide variety of forms: ultra-fine or spherical shaped powders, thin film coatings, ceramic fibers, microporous inorganic membranes, monolithic ceramics and glasses, or extremely porous aerogel materials.

Thin films can be produced on a piece of substrate by spin-coating or dip-coating. When the “sol” is cast into a mold, a wet “gel” will form. With further drying and heat-treatment, the “gel” is converted into dense ceramic or glass articles. The basic sol-gel reaction, shown in Figure 3-18, consists of two chemical reactions that produce a thin film when the sol is applied to a substrate. The first is a hydrolysis reaction and the second is a condensation reaction. The hydrolysis reaction produces the sol, and then, in the condensation reaction, a macroscopic gel is formed on the substrate producing a thin film.

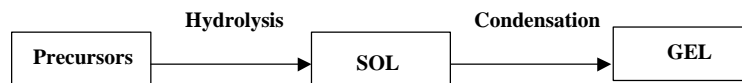


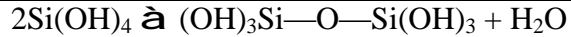
Figure 3-18 Basic sol-gel reaction

This basic sol-gel reaction starts when the metal alkoxide $\text{Si}(\text{OCH}_2\text{CH}_3)_4$ (tetraethoxysilane, or TEOS) is mixed with H_2O and a hydrolysis reaction occurs. TEOS is used because it, along with other metal alkoxides, reacts readily with water. Ethanol is used as a solvent because water and alkoxides are immiscible. Providing there is sufficient water and a catalyst present, the hydrolysis reaction will be completed when all of the $(\text{OCH}_2\text{CH}_3)$ groups are replaced by (OH) :



producing a sol consisting of $\text{Si}(\text{OH})_4$ (silicic acid) and $\text{CH}_3\text{CH}_2\text{OH}$ (ethanol).

Next, two partially hydrolyzed molecules can link together in a condensation reaction that liberates water:



As the reaction proceeds, the number of Si—O—Si bonds increases in a process called polymerization, which produces a macroscopic gel. When producing thin films this gel is formed by rapid evaporation of the solvent.

3.3.2.2 Diaphragm-ferrule bonding

Sol-gel is liquid. It expands, flows and cannot be controlled easily. There are two possible ways to apply sol-gel between the diaphragm and the ferrule. One is spin coating the sol-gel onto the diaphragm. The other way is apply sol-gel onto the ferrule end and keep the diaphragm clean. We finally choose the second way because the spin coated sol-gel layer will also cover the etched pits and contaminate the bottom surface of etched pits.

The whole process of bonding diaphragm and the ferrule is shown as Figure 3-19.

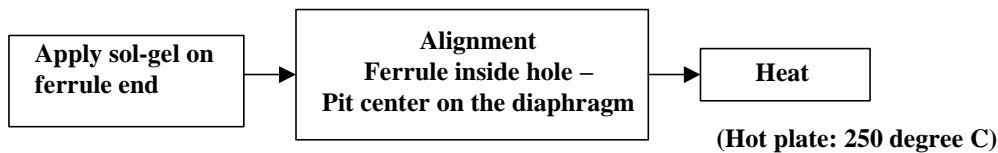


Figure 3-19 Sol-gel bonding process

As we can see from Figure 3-20, the bonding area is the area with sol-gel. The sol-gel area can even be a little bit larger than the etched pit as long as the inside hole of the ferrule is not blocked. A micro-motion three dimensional positioning stage with a monitor system is used to do the alignment. The bonding result is observed under the microscope and is shown as Figure 3-21.

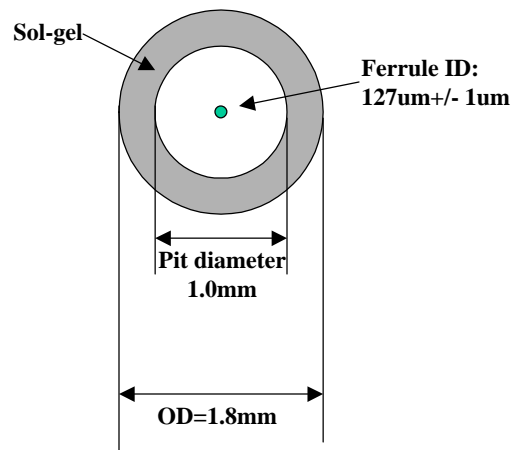


Figure 3-20 Apply sol-gel on the ferrule end



Figure 3-21 Sol-gel bonded diaphragm and ferrule

3.3.2.3 Ferrule-fiber bonding

The last step of the sensor fabrication is to insert the fiber into the ferrule, adjust the air-gap and bond them together. In this step, sol-gel is dip-coated around the surface of the fiber, and heated by using CO₂ laser with very low power for about several seconds. Any heat method, such as the use of a heat gun, a hot plate, a furnace or a laser can work, but after the air-gap adjustment, both the fiber and the ferrule should be kept relatively unmoved on the positioning system during the heating. Because of this requirement, the CO₂ laser based heating method is adopted.

3.4 Sensor fabrication

3.4.1 Principle of White light interferometric Sensor Cavity length Monitoring System

In the process of the sensor fabrication, we use the white light fiber interferometric system, which was developed by the Center of Photonics Technology (CPT), to monitor the length of the interference cavity. The measurement of the sensor cavity length is achieved by demodulating the interference spectrum of the SCIIB sensor.

The basic principle of the white light interferometric sensor cavity length monitoring can be illustrated using Figure 3-22. When the sensor is fabricated, the fiber end and the diaphragm surface will generate an interference signal which is transmitted back to the spectrometer through a 2x2 fiber coupler.

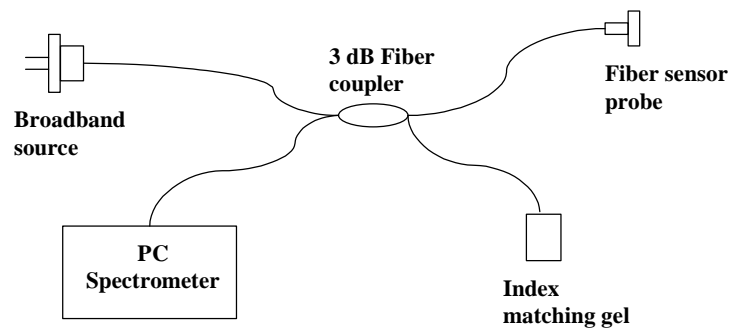


Figure 3-22 Basic principle of the white light interferometric sensor cavity length monitoring

If we assume that the broadband light source (LED or SLED) has a Gaussian spectral power distribution given by

$$I_s(I) = I_0 \exp\left[\frac{-(I - I_0)^2}{(\Delta I)^2}\right] \quad (3-1)$$

where I_0 is the central wavelength, I_0 is the peak value, and ΔI is the source spectral width. The output interference signal is then given by:

$$I = 2I_s \left[1 + g(L) \cos\left(\frac{4pL}{I} + j_0\right) \right] \quad (3-2)$$

where the factor g takes into account the decreased visibility due to the numerical aperture of the fiber as well as other attenuating effects, and j_0 is the initial phase difference between the two interference signals.

If we normalized the interference spectrum given by Equation (3-2) with respect to the source spectrum, we have the normalized interference output expressed as

$$I = 2 \left[1 + g(L) \cos\left(\frac{4pL}{I} + j_0\right) \right] \quad (3-3)$$

It is shown in Equation (3-3) that the output spectrum of the sensor is modulated by a sinusoidal function due to the interference. Because the interference spectrum is a function of the sensor cavity length L , the successful demodulation of this spectral signal can render an accurate and absolute measurement of the sensor cavity length.

A simple case can be considered in which two different spectral components of the source (λ_1 and λ_2) are utilized. These two wavelength components arrive at the spectrometer with different phases, which can be expressed as

$$\begin{aligned} j_1 &= \frac{4pL}{I_1} + j_0 \\ j_2 &= \frac{4pL}{I_2} + j_0 \end{aligned} \quad (3-4)$$

Thus the phase difference between these two spectral components is given by

$$\Delta j = j_1 - j_2 = \frac{4pL(I_1 - I_2)}{I_1 \times I_2} \quad \Delta j = j_1 - j_2 = \frac{4pL(I_1 - I_2)}{I_1 \times I_2} \quad (3-5)$$

Rewriting Equation (3-5), we have

$$L = \frac{\Delta j \times I_1 \times I_2}{4p(I_1 - I_2)} \quad L = \frac{\Delta j \times I_1 \times I_2}{4p(I_1 - I_2)} \quad (3-6)$$

Although it is not easy to measure the phase difference of two arbitrary spectral components, there exist a few special points with fixed phase relation. For example, the phase difference between two adjacent peaks (or valleys) is 2π . Therefore, by detecting the spectral locations of the peaks or valleys in the interference spectrum, we can obtain the cavity length L by applying Equation (3-6).

3.4.2 Diaphragm based pressure sensor

The sensor fabrication is supported by monitoring a single mode fiber white light interferometric system. The source used in the single-mode fiber system is an SLED (EG&G Canada) pigtailed with 9/125 μm single-mode fiber with the central wavelength of 850 nm and the spectral width 20nm. The spectrometer used is a fiber optic PC plug-in spectrometer (PC2000 manufactured by Ocean Optics, Inc.). The PC-2000 spectrometer card uses a 600-line holographic grating to diffract the input light to a CCD array, and interfaces with the computer using a 12-bit A/D converter through the ISA bus. The blaze wavelength is 850nm, and the best efficiency is from 750nm to 950nm, which covers the whole light source spectrum of interest.

For a single-mode fiber Fabry-Perot sensor, the visibility can reach as high as 95% to 99% as shown in Figure 3-23. These two plots were copied from the white light interferometric system. The left plot shows the interference fringes. The right plot shows the normalized interference fringes. The cavity length (also called air-gap) and the interference fringe visibility can be read directly from the right plot. For this sensor, the air-gap is 19.2682 μm .

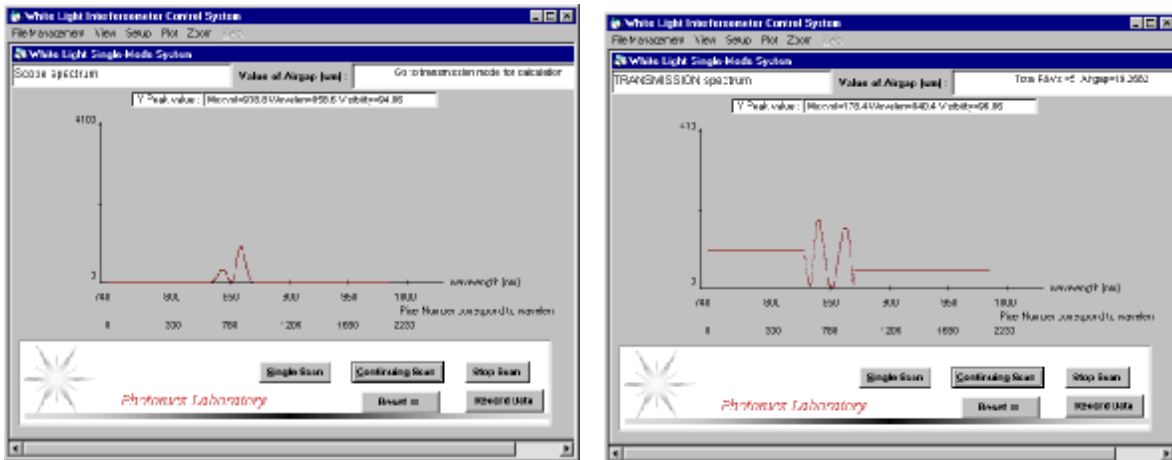


Figure 3-23 White-light interferometric signal